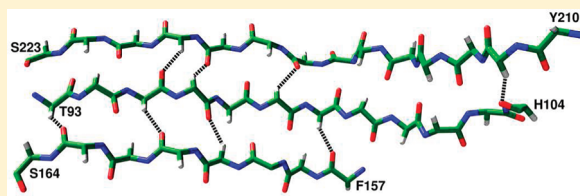


Dynamics of Noncovalent Interactions in All- α and All- β Class Proteins: Implications for the Stability of Amyloid Aggregates

Alok Jain[†] and Ramasubbu Sankararamakrishnan^{*,†}

[†]Department of Biological Sciences and Bioengineering, Indian Institute of Technology Kanpur, Kanpur – 208016, India

ABSTRACT: A fully folded functional protein is stabilized by several noncovalent interactions. When a protein undergoes conformational motions, the existing noncovalent interactions may be maintained. They may also break or new interactions may be formed. Knowledge of the dynamical nature of the different types of noncovalent interactions is extremely important to understand the structural stability, function, and folding of a protein. There are experimental limitations to investigate the dynamics of different noncovalent interactions simultaneously in a biomolecule. We have carried out molecular dynamics simulations on four different proteins, two belonging to all- α class proteins and the other two are representatives of all- β class proteins. The dynamical nature of eight different noncovalent interactions was studied by monitoring the maximum residence time (MRT) and lifetime (LT). The conventional hydrogen bonds are the dominant interactions in all four proteins, and the majority of those formed between the main-chain atoms were maintained during most of the simulation time with MRT greater than 10 ns. Such interactions with more than 1 ns lifetime provide stability to the secondary structures, and hence they are responsible for the overall stability of the protein. The weak C–H \cdots O hydrogen bond is the next major type of interactions. However, a large number of such interactions are observed between the main-chain atoms only in all- β proteins as interstrand interactions, and, surprisingly, they are observed during most part of the simulation although their average lifetime is only about 20 to 30 ps. The strong cation \cdots π and salt-bridge interactions are present few in number. However, in many cases they are almost uninterrupted indicating the higher strength of these interactions. Four other interactions involving the π -electron cloud of aromatic rings are very small in number, and, in many cases, their presence is not maintained throughout the simulation. Our results clearly indicate that the weak C–H \cdots O interactions between the main-chain atoms are the distinguishing factor between the all- α and all- β class of proteins, and these interstrand interactions can provide additional stability to all- β protein structures. Based on these results, we hypothesize that such weak C–H \cdots O interstrand interactions could play a major role in providing stability to amyloid type of aggregates that are responsible for the pathological state of many proteins.



INTRODUCTION

Stable or dynamic nature of noncovalent interactions can play a significant role in the conformation of a protein and its function. Apart from the conventional hydrogen bond and van der Waals interactions, several other types of noncovalent interactions have been shown to be structurally and/or functionally important. For example, it has been shown that the interface in protein–protein interactions is governed by weak noncovalent interactions.¹ The C–H \cdots O hydrogen bonds have been identified to be invariably present in the catalytic triad of all serine hydrolase structures.² Such nonconventional hydrogen bonds have been shown to occur in RNA structures,³ DNA double helices,⁴ and in secondary structures of proteins.^{5–7} Salt-bridges are known to influence the function of proteins,^{8–10} large scale domain motions,¹¹ and regulation of protein–protein interactions.¹² Interactions involving the π electron cloud of aromatic residues seem to play a wide-range of roles in proteins. Analysis of high-resolution protein structures revealed examples of proteins in which many C–H \cdots π interactions are present. In the small C-terminal domain of γ B eye-lens Crystallin protein, as many as 15 C–H \cdots π interactions have been identified indicating their role in providing overall stability to the protein.¹³ The graph spectral

method helped to identify additional clusters of aromatic residues, and it is suggested that the interactions due to these clusters contribute to the additional stability to the thermophilic proteins.¹⁴ In the protein jacalin, a member of the lectin family, the O–H \cdots π and C–H \cdots π interactions have been shown to be involved in the recognition of carbohydrates in jacalin.¹⁵ Crystal structure analysis and *ab initio* quantum chemical calculations indicate that lone-pair \cdots π interactions provide additional stability for the helical segments and are present between water molecules and aromatic residues of protein structures.^{16,17} The role of cation \cdots π interactions in ligand recognition,^{18–22} protein structure stability,^{23,24} and ion transport in channel proteins^{25–28} is well established by several research groups.

The strength of different noncovalent interactions has been determined using *ab initio* quantum chemical calculations on model compounds, gas-phase studies, and other experimental techniques.^{29–33} The energy varies from -1 kcal/mol for the weak C–H \cdots π interactions to -5 to -15 kcal/mol for the strong cation \cdots π and salt-bridge interactions. However to our

Received: July 2, 2011

Published: October 21, 2011

Table 1. Details of the Proteins and the Quality of Their Structures Selected for This Study

	1FAZ	1UJ8	1UAI	1NOA
function	phospholipase A2	unknown	alginate lyase	antibacterial protein
source	<i>Streptomyces violaceoruber</i>	<i>Escherichia coli</i>	<i>Corynebacterium sp.</i>	<i>Streptomyces carzinostaticus</i>
length ^a	122	73	223	113
UniProt ID	Q9Z4W2	P0C0L9	Q9RB42	P0A3R9
resolution	1.4 Å	1.75 Å	1.2 Å	1.5 Å
R-factor	18.8	19.4	17.0	17.2
structural classification ^b	all- α	all- α	all- β	all- β
residues in the disallowed region ^c	0.0%	0.0%	0.5%	0.0%
$\langle G\text{-factor} \rangle$ for dihedral angles ^d	0.37	0.35	0.02	0.10
$\langle G\text{-factor} \rangle$ for main-chain covalent forces ^e	0.53	0.57	0.49	-0.44

^a Polypeptide chain length as available in PDB given in terms of number of amino acids. ^b As per the SCOP classification. ^c Percentage of nonglycine and nonproline residues in the disallowed region of Ramachandran map calculated using PROCHECK.⁵² ^d Average G-factor value calculated for the main-chain and side-chain dihedral angles using the program PROCHECK.⁵² Since all the values are above -0.5, there is no unusual dihedral property for any of the four structures. ^e Average G-factor value calculated for the main-chain bond lengths and main-chain bond angles using the program PROCHECK.⁵² Since all the values are above -0.5, there is no unusual property in the main-chain covalent forces.

knowledge, there is no single study which attempted to compare all the different recognized noncovalent interactions within the same biomolecule and investigated the dynamic nature of different types of interactions. For example, the formation and rupture of hydrogen bonds in liquid water have been investigated using computer simulations and spectroscopy techniques.^{34–38} Understanding the liquid properties of water requires knowledge of water hydrogen bond network, dynamics, and kinetics. Biomolecules are in constant motion, even at very low temperature. This motion can be of different types, namely, vibrational motion at the atomic level due to thermal fluctuations, motion due to side chain movement, or large scale domain motions.³⁹ During such motion, some new noncovalent interactions can be formed, and a number of existing interactions may be broken. Such behavior defines stability of a system in a dynamic environment. These changes significantly depend upon the interaction energy and the nature or environment of the interacting residues. Studies on noncovalent interactions will clearly help to define the role of different interactions in the structure and function of biomolecules. It will also aid to clearly define the contribution of specific interactions in the dynamics and function of biomolecules. Due to experimental constraints and limitations, extensive comparison of different noncovalent interactions within the same molecule has not become possible. Among the few studies reported on the dynamic properties, the approach has been predominantly computational and mainly focusing on interaction in a specific protein or model peptide.^{16,40–43} Moreover, it is to be noted that analyzing the dynamic properties such as lifetime of these interactions through experimental studies is a challenging task.⁴⁴ Using computer simulations, one can investigate the dynamics of different noncovalent interactions simultaneously present in the same molecule, and comparison among different interactions is likely to cast light on the mechanism of the function of such biomolecules.

In this paper, we have compared the dynamical properties of eight different noncovalent interactions in four different proteins. These proteins belong to two different structural classes (all- α and all- β), and molecular dynamics simulations for a period of 30 ns have been carried out for each protein. We have monitored two parameters, namely maximum residence time (MRT) and lifetime (LT), for each interaction and compared with other interactions. The dynamic properties of different interactions are

also compared within and across the different structural classes of proteins. Our analysis clearly reveals the presence of a significantly large number of interstrand C–H···O interactions in β -class of proteins, and many of them exhibit stability over a long period of time. Results of this study could help in understanding the factors that result in extra stability of some of the amyloid aggregates.

METHODS

Four proteins (resolution <1.8 Å; R-factor <20) were downloaded from the Protein Data Bank (<http://www.pdb.org/>).⁴⁵ Two of them belong to all- α class (PDB ID: 1FAZ⁴⁶ and 1UJ8⁴⁷) and the other two are from all- β class (PDB ID: 1UAI⁴⁸ and 1NOA⁴⁹) as per the SCOP classification (<http://scop.berkeley.edu/>).^{50,51} The occupancy of all atoms is one, and the selection of the four proteins is also based on the fact that they do not have any cofactors and their size is reasonably small (77 to 224 residues). The quality of protein structures was checked by examining various parameters using the program PROCHECK.⁵² The functions of the selected proteins are also different. Two of them are enzymes (1FAZ and 1UAI), one is a hypothetical protein (1UJ8), and 1NOA is an antitumor and antibiotic protein. Details of all the four selected proteins are summarized in Table 1, and their schematic diagrams are shown in Figure 1.

The geometrical parameters used to define the eight different noncovalent interactions are presented in Figure 2 and Table 2.^{6,16,24,53–55} In-house perl scripts were developed to identify the interactions present in the crystal structures. The identified interactions were divided into three categories, namely, main-chain···main-chain (MC-MC), main-chain···side-chain (MC-SC), and side-chain···side-chain (SC-SC) depending upon the interacting atoms. We have followed the time evolution of each interaction identified in the crystal structures. We have also identified newly formed interactions as the system evolved during the 30 ns simulation of each protein.

Molecular Dynamics Simulations. Classical molecular dynamics simulations were performed with the GROMACS 3.2.1 package using the OPLS-AA force field.^{56,57} Hydrogen atoms were added using the pdb2gmx module of the GROMACS suite. The starting structures of all four proteins were embedded in the center of a cubical box where the distance between the solute and

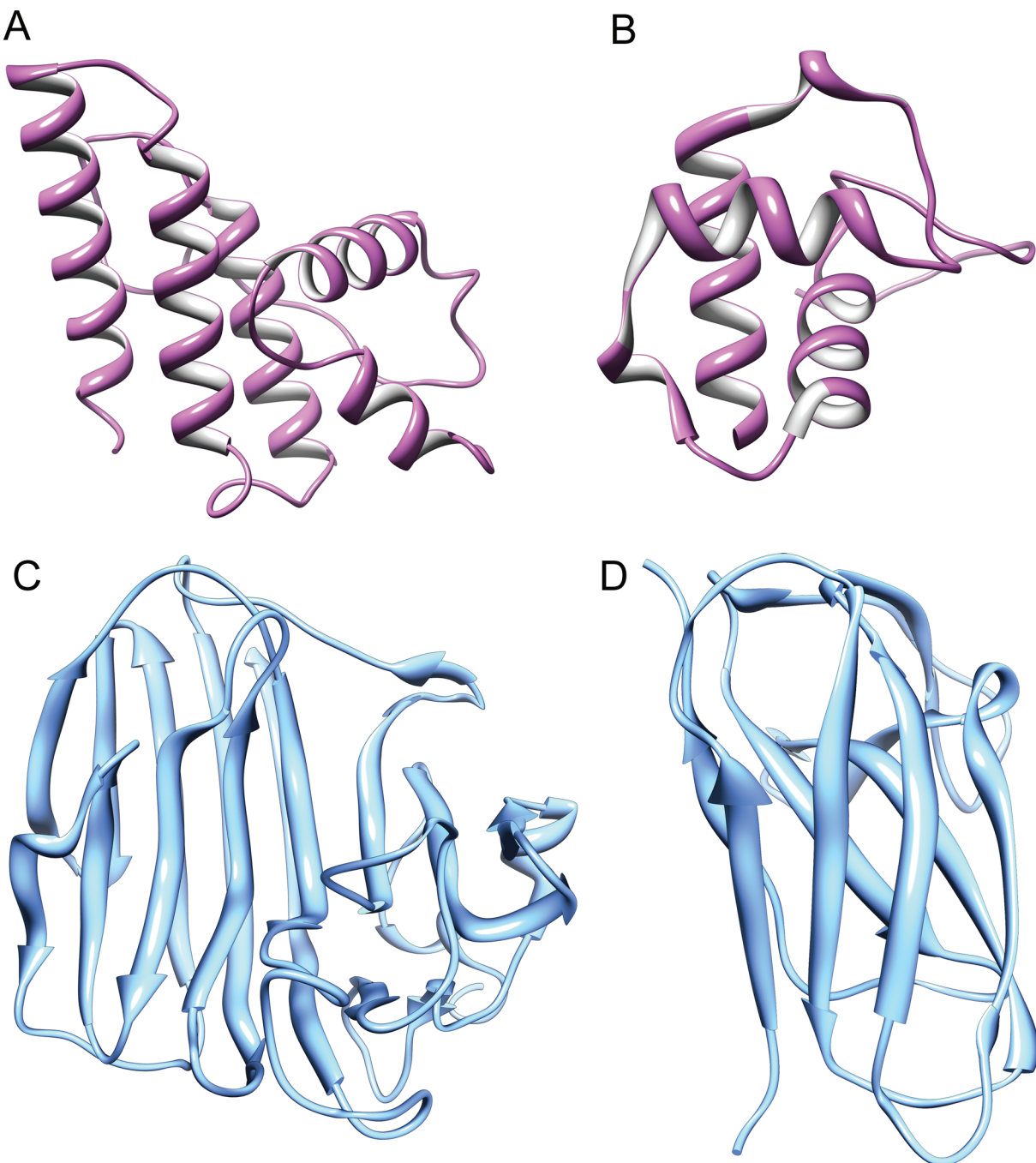


Figure 1. The ribbon diagram of the four representative protein structures used in the present study. They are referred by their unique PDB IDs, namely, (A) 1FAZ, (B) 1UJ8, (C) 1UAI, and (D) 1NOA. This figure and subsequent molecular plots were created using UCSF Chimera package.⁷⁶

the edge of the box was at least 15 Å. The TIP3P water model was used for solvation.^{58,59} Counter ions were added to neutralize the system if needed. The total number of atoms in the system varied from 35266 to 56006. In all the simulations, periodic boundary conditions (PBC) were employed in all three directions. The solvated structure was first energy minimized using the steepest descent method, followed by conjugate gradient. Following minimization, MD equilibration run was performed in two stages, initially with position restraints on the solute atoms for 1 ns using the NVT ensemble. In the latter half of equilibration, these restraints were removed and another 1 ns run was carried out using

the NPT ensemble. Finally the 30 ns MD run was initiated using the NPT ensemble which was considered as the production phase. The emergent trajectory was used for further analysis. Berendsen's coupling algorithm was used for keeping the temperature and pressure constant ($P = 1$ bar, $\tau_p = 1$ ps, $T = 300$ K, $\tau_T = 0.05$ ps).⁶⁰ The temperature bath was separately coupled to the solute and the solvent. Long range nonbonded interactions were evaluated using the PME method and VDW interactions were calculated using a twin range spherical cutoff of 12 Å and 10 Å.⁶¹ A time step of 2 fs was used with the nonbonded list update at every 10 steps together with the interactions within the

long-range cutoff, whereas interactions within the short-range cutoff were updated every time step and the coordinates were saved every 1 ps. During the MD run, LINCS algorithm was used to constrain the bonds involving hydrogen atoms.⁶² Equations of motion for the water atoms were solved analytically with the SETTLE algorithm.⁶³

Dynamics of Noncovalent Interactions. We have analyzed two parameters, maximum residence time (MRT) and lifetime (LT), of all the noncovalent interactions belonging to eight different types for each protein. MRT is the fraction of simulation time for which a specific interaction is maintained, and it has been used to understand the dynamics of water interactions with proteins like ribonuclease A, angiogenin, and the trp-repressor operator complex.^{64,65} A specific interaction is said to be observed when it satisfies all the geometric criteria as defined in Figure 2 and Table 2. Comparison of MRT for different noncovalent interactions will give an idea about relative stability and dynamics of a particular interaction with respect to others, and it is the amount of time a specific interaction is observed within the 30 ns simulation period. Lifetime (LT) is another parameter which is used to find the longest time period in which a specific interaction is maintained without any disruption during the course of 30 ns simulation. The difference between MRT and LT is that an interaction having an MRT of 20 ns indicates that this interaction is observed in 20 out of 30 ns simulation period but need not be present continuously. An interaction with LT 20 ns implies that this is present continuously for a period of 20 ns in a 30 ns

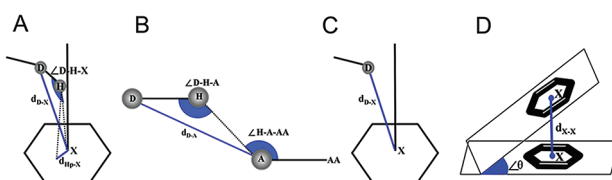


Figure 2. Geometrical parameters that are used to define different noncovalent interactions: (A) C-H...π and D-H...π; (B) D-H...A and C-H...O; (C) LP...π and cation...π; and (D) π...π interactions. The symbol 'X' represents the center of aromatic moiety. Distance between donor atoms (O, N, and C) and the aromatic center is denoted as d_{D-X} . The symbol representing the distance between two aromatic centers is d_{X-X} . D-H...X, D-H...A, H-A...AA represent the angles between donor-hydrogen-aromatic center, donor-hydrogen-acceptor, and hydrogen-acceptor-acceptor antecedent respectively. θ denotes the angle between two aromatic planes.

Table 2. Geometrical Parameters To Define Different Noncovalent Interactions

interaction	criteria used to define an interaction ^a	reference
cation...π	$d_{D-X} \leq 6.0 \text{ \AA}$	Gallivan and Dougherty (1999) ²⁴
C-H...O	$d_{D-A} \leq 3.5 \text{ \AA}$; $\phi(D-H\cdots A) \geq 120^\circ$	Weiss et al. (2001) ⁵³
C-H...π	$d_{D-X} \leq 4.5 \text{ \AA}$; $\phi(D-H\cdots X) \geq 120^\circ$; $d_{Hp-X} \leq 1.2 \text{ (1.0)c \AA}$	Weiss et al. (2001) ⁵³
D-H...A	$d_{D-A} \leq 3.5 \text{ \AA}$; $\phi(D-H\cdots A) \geq 90^\circ$; $\phi(H\cdots A-AA) \geq 90^\circ$	Weiss et al. (2001) ⁵³
D-H...π	$d_{D-X} \leq 4.3 \text{ \AA}$; $\phi(D-H\cdots X) \geq 120^\circ$; $d_{Hp-X} \leq 1.2 \text{ (1.0)c \AA}$	Weiss et al. (2001) ⁵³
LP...π	$d_{D-X} \leq 3.5 \text{ \AA}$	Jain et al. (2007) ¹⁶
salt-bridge ^b	$d_{D-A} \leq 4.0 \text{ \AA}$	Kumar et al. (2000) ⁵⁴
π...π ^d	$d_{X-X} \leq 6.0 \text{ \AA}$; $\theta \leq 30^\circ$	Samanta et al. (1999) ⁵⁵ and Bhattacharyya et al. (2002) ⁶

^a For explanation of different symbols, see Figure 2. ^b For salt-bridge interaction, d_{D-A} indicates the minimum distance between the side-chain functional groups of Arg/Lys/His and the side-chain carboxylic group of Asp/Glu. ^c Values in parentheses are for five-membered rings. ^d A more stringent criteria for the distance between ring centers is used. The angle criteria is used to make sure that the aromatic planes are parallel and the interaction is due to the π-electron cloud of two aromatic rings.

simulation time. It is possible that an interaction can have MRT 20 ns and LT 10 ns.

RESULTS

MD simulations of all four proteins were analyzed as described in the Methods section. MRT and LT of each interaction were determined. The results are summarized for each protein in Tables 3 and 4. In the 30 ns MD simulation, we have defined an interaction is stable if its MRT is at least one-third of the total simulation time. Interactions were separately analyzed for each category (MC-MC, MC-SC and SC-SC).

Interactions in the Crystal Structures. Among the eight noncovalent interactions, the conventional hydrogen bond of type D-H...A occurs predominantly (Tables 3 and 4). This is not surprising because they are involved in the formation and maintenance of the secondary structures in each protein, and hence D-H...A interactions are most frequently observed between two main chain atoms (MC-MC type). The next dominant interaction is C-H...O type of weak hydrogen bonds. While in all-α class proteins, they occur mostly between main-chain and side-chain atoms (MC-SC), in all-β proteins significant number of them are observed between the main-chain atoms (MC-MC). D-H...π, lp...π, and π...π interactions

Table 3. D-H...A and C-H...O Noncovalent Interactions Identified in the Crystal Structures and the Fraction of These Interactions Which Are Considered Stable (MRT > 10 ns)

interaction ^a	protein ^b	MC-MC ^c	MC-SC ^c	SC-SC ^c	total ^c
D-H...A	1FAZ	110 (87)	35 (20)	21 (14)	166 (121)
	1UJ8	51 (46)	17 (6)	7 (1)	75 (53)
	1UAI	138 (116)	57 (30)	30 (10)	225 (156)
	1NOA	66 (58)	19 (9)	6 (5)	91 (72)
C-H...O	1FAZ	0 (0)	59 (14)	6 (0)	65 (14)
	1UJ8	2 (0)	31 (11)	8 (0)	41 (11)
	1UAI	54 (30)	76 (11)	12 (0)	142 (41)
	1NOA	35 (27)	16 (3)	2 (0)	53 (30)

^a The geometric criteria used to define the interaction are given in Figure 2 and Table 2. These interactions could be due to main-chain...main-chain (MC-MC), main-chain...side-chain (MC-SC), or side-chain...side-chain (SC-SC) atoms. ^b The four letter unique PDB ID of the protein is given. ^c The number of interactions identified in the crystal structures. Those which are considered stable with MRT > 10 ns are given in brackets.

Table 4. Noncovalent Interactions Due to Aromatic Rings and Charged Side-Chains Identified in the Crystal Structures and the Fraction of Those Which Are Considered As Stable (MRT > 10 ns)

interaction ^a	1FAZ ^{b,c}	1UJ8 ^{b,c}	1UAI ^{b,c}	1NOA ^{b,c}
cation···π	9 (5)	0 (0)	7 (5)	0 (0)
C–H···π	19 (3)	7 (1)	19 (5)	7 (2)
D–H···π	1 (1)	1 (1)	1 (1)	0 (0)
LP···π	0 (0)	3 (0)	5 (1)	0 (0)
π···π	3 (3)	1 (0)	8 (1)	0 (0)
salt-bridge	7 (7)	8 (2)	10 (6)	3 (2)

^aThe geometric criteria used to define the interaction are given in Figure 2 and Table 2. These interactions occur between the main-chain···side-chain (MC-SC) and side-chain···side-chain (SC-SC) atoms. ^bThe four letter unique PDB ID of the protein is given. ^cThe number of interactions identified in the crystal structures. Those which are considered stable with MRT > 10 ns are given in brackets.

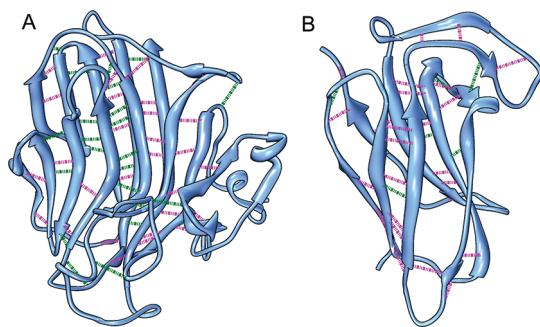


Figure 3. The C–H···O interstrand interactions that occur between the main-chain atoms in the all-β class of proteins (A) 1UAI and (B) 1NOA. C–H···O interactions shown in pink are stable and have MRT > 10 ns, while those shown in green have MRT less than 10 ns.

are the least frequently observed, while C–H···π interactions are relatively more and they occur mostly between side-chain atoms (Table 4). The strong cation···π and salt-bridge interactions are minimum in number perhaps due to the fact that a large number of such interactions will make proteins extremely rigid which may be detrimental to its function.

Interactions with MRT More than 10 ns. The number of interactions which maintain an MRT of greater than 10 ns is given in brackets in Tables 3 and 4. It is clear that a large number of conventional hydrogen bonds (D–H···A) have MRT 10 ns or more, and this is especially true for those that belong to MC-MC category. This is understandable since the structural integrity of a protein depends upon the overall stability of its secondary structure. In fact, more than 50% of D–H···A interactions have MRT > 20 ns.

The next major interaction, namely C–H···O, shows a distinct pattern of stability for all-α and all-β proteins. In all-α where the majority of this interaction occurs between the main-chain and side-chain atoms, only a fraction of them with MRT > 10 ns can be considered as stable. Interestingly in all-β proteins, a large number of C–H···O interactions occurring between two main-chain atoms remains stable. Closer examination of these proteins indicates that these are interstrand interactions, and perhaps they are involved in the stabilization of protein structures. The main-chain···main-chain C–H···O interactions in

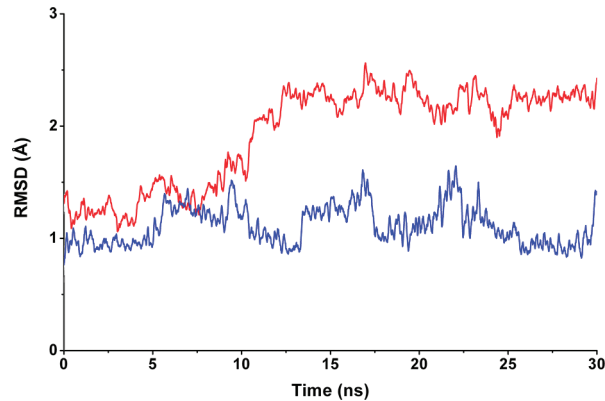


Figure 4. Root mean square deviation (RMSD) profiles of two representative proteins, one from all-α (PDB ID: 1FAZ; red) and the other from all-β (PDB ID: 1NOA; blue). Only the Cα atoms were used to calculate the RMSD between the starting structure and the MD-simulated structure.

Table 5. New Noncovalent Interactions Formed during the Simulations and Those Which Are Considered Stable with MRT > 10 ns

interaction ^a	1FAZ ^{b,c}	1UJ8 ^{b,c}	1UAI ^{b,c}	1NOA ^{b,c}
D–H···A	337 (32)	214 (15)	616 (43)	261 (18)
C–H···O	442 (21)	280 (15)	893 (27)	370 (14)
cation···π	5 (0)	4 (0)	12 (2)	1 (0)
C–H···π	57 (5)	40 (1)	61 (9)	17 (2)
D–H···π	11 (0)	12 (0)	14 (1)	3 (0)
LP···π	15 (0)	18 (0)	21 (1)	3 (0)
π···π	23 (1)	9 (0)	13 (0)	0 (0)
salt-bridge	4 (1)	14 (1)	9 (2)	2 (1)

^aThe geometric criteria used to define the interaction are given in Figure 2 and Table 2. These interactions belong to all three categories viz. MC-MC, MC-SC, and SC-SC. ^bThe four letter unique PDB ID of the protein is given. ^cThe number of new interactions evolved during the course of simulation. Those which are considered stable with MRT > 10 ns are given in brackets.

the two all-β class proteins are shown in Figure 3. The stable C–H···O interactions with MRT > 10 ns are mostly of interstrand in nature and are observed throughout the protein structures. On the other hand, the C–H···O interactions between the main-chain atoms that have MRT < 10 ns are found to occur in the loop regions or at the end of two interacting β-strands. This clearly illustrates the role of stable interstrand C–H···O interactions implicating them in the stability of overall protein structure.

Although small in number, some of the cation···π and salt-bridge interactions are extremely highly stable with MRT ranging from 20 to 30 ns (Table 4). It must be mentioned that the stabilization energy of cation···π and salt-bridge interactions are as high as –5 to –15 kcal/mol which are several fold more stable than a conventional hydrogen bond.^{66–69} Very few interactions belonging to the other type have MRT more than 10 ns.

RMSD Analysis. We have also plotted the root-mean-square deviation (RMSD) profile of all four proteins as a function of time. RMSD for each MD simulated structure was calculated with respect to the crystal structure by considering all the Cα

Table 6. Average Lifetime (in ns) of Noncovalent Interactions Which Have MRT Greater than 10 ns

interaction ^a	1FAZ ^{b,c}	1UJ8 ^{b,c}	1UAI ^{b,c}	1NOA ^{b,c}
D-H···A	1.75	0.95	3.14	1.94
C-H···O	0.02	0.02	0.03	0.02
cation···π	1.63	N/A	20.97	N/A
C-H···π	0.03	0.06	0.04	0.04
D-H···π	0.08	0.02	0.02	N/A
LP···π	N/A	N/A	0.06	N/A
π···π	0.06	N/A	0.07	N/A
salt-bridge	14.98	7.55	4.12	10.63

^aThe geometric criteria used to define the interaction are given in Figure 2 and Table 2. These interactions belong to all three categories viz. MC-MC, MC-SC and SC-SC. ^bThe four letter unique PDB ID of the protein is given. ^cN/A — not applicable indicating that zero interaction of a particular type has been found with MRT > 10 ns and hence lifetime could not be evaluated.

atoms. RMSD profiles of two representative proteins, one from all- α and the other from all- β , are shown in Figure 4, and these proteins are of comparable size (122 and 113 residues). It is very clearly evident that all- β class of protein is relatively more stable compared to that of all- α protein, and this stability could be clearly attributed to the stable interstrand C-H···O interactions. A similar trend is observed for the other two proteins also (data not shown).

New Interactions That Appear during the Simulation.

During the course of the simulation, some new interactions are also formed which were not observed in the crystal structure. We have also identified them and evaluated the MRT of each new interaction. It is clear that in all four cases, a large number of new D-H···A type of interactions is formed as the simulation progressed (Table 5). It is also interesting to note that an even larger number of new C-H···O interactions is formed during the simulations. It can be seen that although many new noncovalent interactions involving the π electron cloud of aromatic rings are formed, the number of such interactions is very small compared to D-H···A or C-H···O interactions. The same conclusion is true for newly formed salt-bridge interactions also. We have also determined the number of new interactions formed within the first 5 ns. We have observed that a majority of 70 to 90% of new interactions are formed within the first 5 ns. However, only a small number of them have MRT more than 10 ns (Table 5) indicating that most of the newly formed interactions are transient in nature.

Life Time of Noncovalent Interactions.

We have calculated the lifetime of those interactions which have MRT more than 10 ns. The results of lifetime analysis are presented in Table 6. Salt-bridge interactions exhibit the highest average lifetime ranging from 4 to 15 ns. Once formed, salt-bridges can remain uninterrupted for a long time, and this is also evident from the higher strength of the interaction.^{68,69} The other strong interaction, cation···π, also shows a longer average lifetime. In the case of 1UAI simulation, the average lifetime of five cation···π interactions is nearly 21 ns. However, the protein 1FAZ with the same number of cation···π interactions (with MRT > 10 ns) exhibited a smaller average lifetime of 1.63 ns. The average lifetime of the conventional hydrogen bond interactions of D-H···A type varies from ~1 to 3 ns. The average lifetime of all other noncovalent interactions is less than 100 ps. Although a

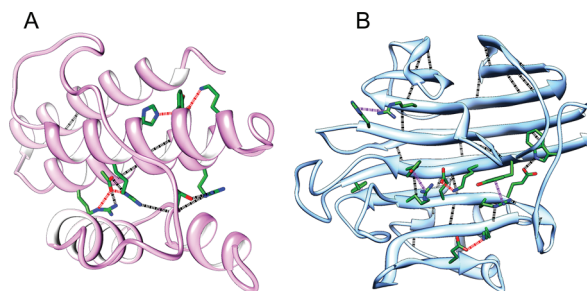


Figure 5. Interactions having long MRT (>25 ns) and LT (>5 ns) are shown for (A) 1FAZ and (B) 1UAI representative proteins for all- α and all- β class respectively. The salt-bridges and cation···π interactions are shown in dashed lines in red and purple colors respectively. The conventional hydrogen bonds are displayed in black dashed lines.

large number of C-H···O interactions exist with MRT > 10 ns, the average lifetime of C-H···O interactions is between 20 and 30 ps. This indicates that due to the weak nature of this interaction, C-H···O interactions can easily form and break. In fact, the lifetime of C-H···O interaction is comparable to that of hydrogen bonds present in liquid water.⁷⁰ However, when several C-H···O interactions are present in a molecule, they together can provide overall stability which is reinforced by that fact that a significantly large number of them have MRT > 10 ns in two out of four proteins investigated in this study.

Interactions with MRT > 25 ns and LT at least 5 ns are shown in Figure 5 for the proteins 1FAZ and 1UAI. For the all- α protein 1FAZ, 11 D-H···A conventional hydrogen bonds and 4 salt-bridges are observed in this category (Figure 5A). Most of them are intra- or interhelical interactions. Stable intrahelical interactions strengthen the individual helices, and strong interhelical interactions provide overall stability for the helix packing. Some of the residues participate in more than one type of interactions with multiple residues. It is worth mentioning that residues participating in the majority of these interactions in 1FAZ are contributed by one single helix (formed by residues 81 to 96) which is centrally located.

For the all- β 1UAI protein, 26 D-H···A type of conventional hydrogen bonds, 4 cation···π, and two salt-bridges have both long MRT (more than 25 ns) and LT (more than 5 ns) and a majority of them occur as interstrand interactions. While the cation···π and salt-bridge interactions are of SC-SC type, 24 out of 26 D-H···A interactions occur between the main-chain atoms between two adjacent strands. Unlike the all- α 1FAZ protein, these interactions seem to be spread over the entire protein.

■ DISCUSSION

We have carried out molecular dynamics simulations of four different proteins belonging to all- α class and all- β class according to SCOP classification. We have identified and monitored eight different noncovalent interactions as a function of time. The dynamical nature of these interactions was assessed by calculating two quantities, namely, the maximum residence time and lifetime. Not surprisingly, the noncovalent interactions in the crystal structures are dominated by the D-H···A type of conventional hydrogen bonds. The next major type of interaction is the C-H···O type of weak hydrogen bond. Here, we observe that C-H···O type of interactions due to main-chain atoms (MC-MC type) is almost completely absent in the two α -class

proteins, whereas a significant number of them belonging to the MC-MC category are present in the two all- β class proteins as interstrand interactions. Interactions involving the π -electron cloud of aromatic rings and the salt-bridge interactions are few in number.

A large number of D-H \cdots A interactions (about 70% or more) have MRT more than 10 ns indicating that they are present more than one-third of the total simulation time. The average lifetime of the conventional hydrogen bonds also exceeds 1 ns. The presence of such stable hydrogen bonds gives stability to the secondary structures and thus provides overall stability to the protein structure. Surprisingly, most of the C-H \cdots O interstrand hydrogen bonds are also observed for the major part of the simulation time with MRT greater than 10 ns. Although weak in nature, the presence of several such C-H \cdots O interactions for a longer period of simulation time certainly provides additional stability to the β -sheet structure in all- β class proteins. This is also evident from the RMSD analysis. Due to the weak nature of this interaction, the lifetime of C-H \cdots O hydrogen bond is only a few picoseconds indicating that they are more frequently broken and formed during the simulation. The stronger cation \cdots π and salt-bridge interactions are present few in number. This is obvious since more such interactions will make the protein extremely rigid which may not be desirable for its function. However these strong interactions, if they are present, have long MRT as well as long lifetime. Interactions involving the π -electron cloud of aromatic rings are fewer with only C-H \cdots π interactions more frequently observed. However, the lifetime of these interactions is less than 100 ps.

To our knowledge, this is the first study which compared the dynamic nature of many different types of noncovalent interactions present within the same protein. The comparison is also carried out across four different proteins belonging to two different structural classes. This study clearly implicates the weak C-H \cdots O interstrand interactions that occur between the main-chain atoms in providing extra stability to all- β protein structures. It has been reported that the C-H \cdots O interactions observed in α -helices either occur at the helix termini or they are due to main-chain \cdots side-chain (MC-SC) interactions.⁵ The presence of interstrand C-H \cdots O interactions has been reported earlier.⁷ However, their structural significance in providing additional stability has been unambiguously demonstrated in this study.

The biological importance of this observation can easily be recognized by the fact that the MC-MC C-H \cdots O interaction is clearly a distinguishing factor between all- α and all- β structures. The formation of amyloid aggregates in many proteins is characterized by the presence of β -sheet structures, and they seem to be extremely stable.^{71,72} Several experimental and computational studies have been carried out to find out the factors responsible for the stable nature of amyloid aggregates, and they have suggested electrostatic, hydrophobic, or interstrand side-chain interactions.^{73–75} To our knowledge, none of the studies suggested the role of interstrand C-H \cdots O interactions as an important factor for the amyloid stability. The present simulation studies clearly suggest that the weak C-H \cdots O interstrand interaction could be a major player in stabilizing the amyloid formation and propagation. Our studies suggest that disrupting the interstrand C-H \cdots O hydrogen bonds in amyloid structures is one way to prevent the formation of amyloid aggregates.

■ AUTHOR INFORMATION

Corresponding Author

*Phone: +91 512 259 4014. Fax: +91 512 259 4010. E-mail: rsankar@iitk.ac.in.

■ ACKNOWLEDGMENT

Alok Jain wants to thank Council of Scientific and Industrial Research (CSIR) for a Senior Research Fellowship. We thank the anonymous reviewer for the useful suggestions which improved the manuscript. We would like to thank all our lab members, especially Dilraj Lama and Ravi Kumar Verma for their help and discussions.

■ REFERENCES

- (1) Nooren, I. M. A.; Thornton, J. M. Structural characterisation and functional significance of transient protein-protein interactions. *J. Mol. Biol.* **2003**, *325*, 991–1018.
- (2) Derewenda, Z. S.; Derewenda, U.; Kobos, P. M. (His)C-H \cdots O=C \cdots hydrogen bond in the active sites of serine hydrolases. *J. Mol. Biol.* **1994**, *241*, 83–93.
- (3) Brandl, M.; Lindauer, K.; Meyer, M.; Sühnel, J. C-H..O and C-H..N interactions in RNA structures. *Theor. Chem. Acc.* **1999**, *101*, 103–113.
- (4) Ghosh, A.; Bansal, M. C-H..O hydrogen bonds in minor groove of A-tracts in DNA double helices. *J. Mol. Biol.* **1999**, *294*, 1149–1158.
- (5) Manikandan, K.; Ramakumar, S. The occurrence of C-H..O hydrogen bonds in α -helices and helix termini in globular proteins. *Proteins: Struct., Funct., Bioinf.* **2004**, *56*, 768–781.
- (6) Bhattacharyya, R.; Samanta, U.; Chakrabarti, P. Aromatic–aromatic interactions in and around α -helices. *Protein Eng.* **2002**, *15*, 91–100.
- (7) Ho, B. K.; Curmi, P. M. G. Twist and shear in β -sheets and β -ribbons. *J. Mol. Biol.* **2002**, *317*, 291–308.
- (8) Barouch-Bentov, R.; Che, J.; Lee, C. C.; Yang, Y.; Herman, A.; Jia, Y.; Velentza, A.; Watson, J.; Sternberg, L.; Kim, S.; Ziaeef, N.; Miller, A.; Jackson, C.; Fujimoto, M.; Young, M.; Batalov, S.; Liu, Y.; Warmuth, M.; Wiltshire, T.; Cooke, M. P.; Sauer, K. A conserved salt bridge in the G loop of multiple protein kinases is important for catalysis and for in vivo lyn function. *Mol. Cell* **2009**, *33*, 43–52.
- (9) Mahalingam, M.; Martínez-Mayorga, K.; Brown, M. F.; Vogel, R. Two protonation switches control rhodopsin activation in membranes. *Proc. Natl. Acad. Sci. U. S. A.* **2008**, *105*, 17795–17800.
- (10) Kristiansen, K. Molecular mechanisms of ligand binding, signaling, and regulation within the superfamily of G-protein-coupled receptors: Molecular modeling and mutagenesis approaches to receptor structure and function. *Pharmacol. Ther.* **2004**, *103*, 21–80.
- (11) Stockner, T.; Vogel, H. J.; Tielemans, D. P. A salt-bridge motif involved in ligand binding and large-scale domain motions of the maltose-binding protein. *Biophys. J.* **2005**, *89*, 3362–3371.
- (12) Dehner, A.; Klein, C.; Hansen, S.; Müller, L.; Buchner, J.; Schwaiger, M.; Kessler, H. Cooperative binding of p53 to DNA: Regulation by protein–protein interactions through a double salt bridge. *Angew. Chem., Int. Ed.* **2005**, *44*, 5247–5251.
- (13) Brandl, M.; Weiss, M. S.; Jabs, A.; Suhnel, J.; Hilgenfeld, R. C-H \cdots π interactions in proteins. *J. Mol. Biol.* **2001**, *307*, 357–377.
- (14) Kannan, N.; Vishveshwara, S. Aromatic clusters: A determinant of thermal stability of thermophilic proteins. *Protein Eng.* **2000**, *13*, 753–761.
- (15) Jeyaprakash, A. A.; Katiyar, S.; Swaminathan, C. P.; Sekar, K.; Surolia, A.; Vijayan, M. Structural basis of the carbohydrate specificities of jacalin: An X-ray and modeling study. *J. Mol. Biol.* **2003**, *332*, 217–228.
- (16) Jain, A.; Purohit, C. S.; Verma, S.; Sankaramakrishnan, R. Close contacts between carbonyl oxygen atoms and aromatic centers in

- protein structures: $\pi \cdots \pi$ or lone-pair $\cdots \pi$ interactions? *J. Phys. Chem. B* **2007**, *111*, 8680–8683.
- (17) Jain, A.; Ramanathan, V.; Sankararamakrishnan, R. Lone pair $\cdots \pi$ interactions between water oxygens and aromatic residues: Quantum chemical studies based on high-resolution protein structures and model compounds. *Protein Sci.* **2009**, *18*, 595–605.
- (18) Pless, S. A.; Hanek, A. P.; Price, K. L.; Lynch, J. W.; Lester, H. A.; Dougherty, D. A.; Lummis, S. C. R. A cation- π interaction at a phenylalanine residue in the glycine receptor binding site is conserved for different agonists. *Mol. Pharmacol.* **2011**, *79*, 742–748.
- (19) Pan, Y.; Zhang, K.; Qi, J.; Yue, J.; Springer, T. A.; Chen, J. Cation- π interaction regulates ligand-binding affinity and signaling of integrin $\alpha_4\beta_7$. *Proc. Natl. Acad. Sci. U. S. A.* **2010**, *107*, 21388–21393.
- (20) Queralt-Rosinach, N.; Mestres, J. A canonical cation- π interaction stabilizes the agonist conformation of estrogen-like nuclear receptors. *Eur. Biophys. J.* **2010**, *39*, 1471–1475.
- (21) Tantry, S.; Ding, F.-X.; Dumont, M.; Becker, J. M.; Naider, F. Binding of fluorinated phenylalanine α -factor analogues to ste2p: Evidence for a cation- π binding interaction between a peptide ligand and its cognate G protein-coupled receptor. *Biochemistry* **2010**, *49*, 5007–5015.
- (22) Zacharias, N.; Dougherty, D. A. Cation- π interactions in ligand recognition and catalysis. *Trends Pharmacol. Sci.* **2002**, *23*, 281–287.
- (23) Waters, M. L. Aromatic interactions in peptides: Impact on structure and function. *Pept. Sci.* **2004**, *76*, 435–445.
- (24) Gallivan, J. P.; Dougherty, D. A. Cation- π interactions in structural biology. *Proc. Natl. Acad. Sci. U. S. A.* **1999**, *96*, 9459–9464.
- (25) Santarelli, V. P.; Eastwood, A. L.; Dougherty, D. A.; Horn, R.; Ahern, C. A. A cation- π interaction discriminates among sodium channels that are either sensitive or resistant to tetrodotoxin block. *J. Biol. Chem.* **2007**, *282*, 8044–8051.
- (26) Liu, Y.; Hu, X. Molecular determinants for binding of ammonium ion in the ammonia transporter AmtBA quantum chemical analysis. *J. Phys. Chem. A* **2005**, *110*, 1375–1381.
- (27) Beene, D. L.; Brandt, G. S.; Zhong, W.; Zacharias, N. M.; Lester, H. A.; Dougherty, D. A. Cation- π interactions in ligand recognition by serotonergic (5-HT_{3A}) and nicotinic acetylcholine receptors: The anomalous binding properties of nicotine. *Biochemistry* **2002**, *41*, 10262–10269.
- (28) Santarelli, V. P.; Eastwood, A. L.; Dougherty, D. A.; Ahern, C. A.; Horn, R. Calcium block of single sodium channels: Role of a pore-lining aromatic residue. *Biophys. J.* **2007**, *93*, 2341–2349.
- (29) Cerny, J.; Hobza, P. Non-covalent interactions in biomacromolecules. *Phys. Chem. Chem. Phys.* **2007**, *9*, 5291–5303.
- (30) Mueller-Dethlefs, K.; Hobza, P. Noncovalent interactions: A challenge for experiment and theory. *ChemInform* **2000**, *31*, 143–168.
- (31) Salonen, L. M.; Ellermann, M.; Diederich, F. Aromatic rings in chemical and biological recognition: Energetics and structures. *Angew. Chem., Int. Ed.* **2011**, *50*, 4808–4842.
- (32) Rusconi, F.; Guillonneau, F.; Praseuth, D. Contributions of mass spectrometry in the study of nucleic acid-binding proteins and of nucleic acid–protein interactions. *Mass Spectrom. Rev.* **2002**, *21*, 305–348.
- (33) Yanes, O.; Villanueva, J.; Querol, E.; Aviles, F. X. Detection of non-covalent protein interactions by ‘intensity fading’ MALDI-TOF mass spectrometry: Applications to proteases and protease inhibitors. *Nat. Protoc.* **2007**, *2*, 119–130.
- (34) Luzar, A. Resolving the hydrogen bond dynamics conundrum. *J. Chem. Phys.* **2000**, *113*, 10663–10675.
- (35) Fecko, C. J.; Loparo, J. J.; Roberts, S. T.; Tokmakoff, A. Local hydrogen bonding dynamics and collective reorganization in water: Ultrafast infrared spectroscopy of HOD/D₂O. *J. Chem. Phys.* **2005**, *122*, 54506–54518.
- (36) Asbury, J. B.; Steinle, T.; Kwak, K.; Corcelli, S. A.; Lawrence, C. P.; Skinner, J. L.; Fayer, M. D. Dynamics of water probed with vibrational echo correlation spectroscopy. *J. Chem. Phys.* **2004**, *121*, 12431–12446.
- (37) Nicodemus, R. A.; Corcelli, S. A.; Skinner, J. L.; Tokmakoff, A. Collective hydrogen bond reorganization in water studied with temperature-dependent ultrafast infrared spectroscopy. *J. Phys. Chem. B* **2011**, *115*, S604–S616.
- (38) Voloshin, V.; Naberukhin, Y. Hydrogen bond lifetime distributions in computer-simulated water. *J. Struct. Chem.* **2009**, *50*, 78–89.
- (39) Ding, F.; Dokholyan, N. V. Simple but predictive protein models. *Trends Biotechnol.* **2005**, *23*, 450–455.
- (40) Khandelia, H.; Kaznessis, Y. N. Cation- π interactions stabilize the structure of the antimicrobial peptide indolicidin near membranes: Molecular dynamics simulations. *J. Phys. Chem. B* **2006**, *111*, 242–250.
- (41) Zhang, R.; Li, H.; Lei, Y.; Han, S. All-atom molecular dynamic simulations and relative NMR spectra study of weak C–H \cdots O contacts in amide–water systems. *J. Phys. Chem. B* **2005**, *109*, 7482–7487.
- (42) Guvench, O.; Brooks, C. L. Tryptophan side chain electrostatic interactions determine edge-to-face vs parallel-displaced tryptophan side chain geometries in the designed β -hairpin “trpzip2”. *J. Am. Chem. Soc.* **2005**, *127*, 4668–4674.
- (43) Chelli, R.; Gervasio, F. L.; Procacci, P.; Schettino, V. Stacking and T-shape competition in aromatic–aromatic amino acid interactions. *J. Am. Chem. Soc.* **2002**, *124*, 6133–6143.
- (44) Sigala, P. A.; Tsuchida, M. A.; Herschlag, D. Hydrogen bond dynamics in the active site of photoactive yellow protein. *Proc. Natl. Acad. Sci. U. S. A.* **2009**, *106*, 9232–9237.
- (45) Bernstein, F. C.; Koetzle, T. F.; Williams, G. J. B.; Meyer, J. E. F.; Brice, M. D.; Rodgers, J. R.; Kennard, O.; Shimanouchi, T.; Tasumi, M. The protein data bank: A computer-based archival file for macromolecular structures. *J. Mol. Biol.* **1977**, *112*, 535–542.
- (46) Matoba, Y.; Katsube, Y.; Sugiyama, M. The crystal structure of prokaryotic phospholipase A₂. *J. Biol. Chem.* **2002**, *277*, 20059–20069.
- (47) Shimomura, Y.; Takahashi, Y.; Kakuta, Y.; Fukuyama, K. Crystal structure of escherichia coli YfhJ protein, a member of the ISC machinery involved in assembly of iron–sulfur clusters. *Proteins: Struct., Funct., Bioinf.* **2005**, *60*, S66–S69.
- (48) Osawa, T.; Matsubara, Y.; Muramatsu, T.; Kimura, M.; Kakuta, Y. Crystal structure of the alginate (poly α -l-guluronate) lyase from corynebacterium sp. at 1.2 Å resolution. *J. Mol. Biol.* **2005**, *345*, 1111–1118.
- (49) Teplyakov, A.; Obmolova, G.; Wilson, K.; Kuromizu, K. Crystal structure of apo-neocarzinostatin at 0.15-nm resolution. *Eur. J. Biochem.* **1993**, *213*, 737–741.
- (50) Andreeva, A.; Howorth, D.; Chandonia, J.-M.; Brenner, S. E.; Hubbard, T. J. P.; Chothia, C.; Murzin, A. G. Data growth and its impact on the SCOP database: New developments. *Nucleic Acids Res.* **2008**, *36*, D419–D425.
- (51) Murzin, A. G.; Brenner, S. E.; Hubbard, T.; Chothia, C. SCOP: A structural classification of proteins database for the investigation of sequences and structures. *J. Mol. Biol.* **1995**, *247*, 536–540.
- (52) Laskowski, R. A.; MacArthur, M. W.; Moss, D. S.; Thornton, J. M. PROCHECK: A program to check the stereochemical quality of protein structures. *J. Appl. Crystallogr.* **1993**, *26*, 283–291.
- (53) Weiss, M. S.; Brandl, M.; Süehnel, J.; Pal, D.; Hilgenfeld, R. More hydrogen bonds for the (structural) biologist. *Trends Biochem. Sci.* **2001**, *26*, S21–S23.
- (54) Kumar, S.; Ma, B.; Tsai, C.-J.; Nussinov, R. Electrostatic strengths of salt bridges in thermophilic and mesophilic glutamate dehydrogenase monomers. *Proteins: Struct., Funct., Bioinf.* **2000**, *38*, 368–383.
- (55) Samanta, U.; Pal, D.; Chakrabarti, P. Packing of aromatic rings against tryptophan residues in proteins. *Acta Crystallogr., Sect. D: Biol. Crystallogr.* **1999**, *55*, 1421–1427.
- (56) Lindahl, E.; Hess, B.; van der Spoel, D. GROMACS 3.0: A package for molecular simulation and trajectory analysis. *J. Mol. Model.* **2001**, *7*, 306–317.
- (57) Jorgensen, W. L.; Maxwell, D. S.; Tirado-Rives, J. Development and testing of the OPLS all-atom force field on conformational energetics and properties of organic liquids. *J. Am. Chem. Soc.* **1996**, *118*, 11225–11236.
- (58) Jorgensen, W. L.; Chandrasekhar, J.; Madura, J. D.; Impey, R. W.; Klein, M. L. Comparison of simple potential functions for simulating liquid water. *J. Chem. Phys.* **1983**, *79*, 926–935.

- (59) Neria, E.; Fischer, S.; Karplus, M. Simulation of activation free energies in molecular systems. *J. Chem. Phys.* **1996**, *105*, 1902–1921.
- (60) Berendsen, H. J. C.; Postma, J. P. M.; van Gunsteren, W. F.; DiNola, A.; Haak, J. R. Molecular dynamics with coupling to an external bath. *J. Chem. Phys.* **1984**, *81*, 3684–3690.
- (61) Essmann, U.; Perera, L.; Berkowitz, M. L.; Darden, T.; Lee, H.; Pedersen, L. G. A smooth particle mesh ewald method. *J. Chem. Phys.* **1995**, *103*, 8577–8593.
- (62) Hess, B.; Bekker, H.; Berendsen, H. J. C.; Fraaije, J. G. E. M. LINCS: A linear constraint solver for molecular simulations. *J. Comput. Chem.* **1997**, *18*, 1463–1472.
- (63) Miyamoto, S.; Kollman, P. A. Settle: An analytical version of the SHAKE and RATTLE algorithm for rigid water models. *J. Comput. Chem.* **1992**, *13*, 952–962.
- (64) Sanjeev, B. S.; Vishveshwara, S. Protein–water interactions in ribonuclease A and angiogenin: A molecular dynamics study. *Proteins: Struct., Funct., Bioinf.* **2004**, *55*, 915–923.
- (65) Wibowo, F. R.; Rauch, C.; Trieb, M.; Wellenzohn, B.; Liedl, K. R. Water-mediated contacts in the trp-repressor operator complex recognition process. *Biopolymers* **2004**, *73*, 668–681.
- (66) Biot, C.; Buisine, E.; Kwasigroch, J.-M.; Wintjens, R.; Rooman, M. Probing the energetic and structural role of amino acid/nucleobase cation- π interactions in protein-ligand complexes. *J. Biol. Chem.* **2002**, *277*, 40816–40822.
- (67) Gromiha, M. M.; Santhosh, C.; Ahmad, S. Structural analysis of cation- π interactions in DNA binding proteins. *Int. J. Biol. Macromol.* **2004**, *34*, 203–211.
- (68) Hong, H.; Szabo, G.; Tamm, L. K. Electrostatic couplings in OmpA ion-channel gating suggest a mechanism for pore opening. *Nat. Chem. Biol.* **2006**, *2*, 627–635.
- (69) Honig, B. H.; Hubbell, W. L. Stability of "salt bridges" in membrane proteins. *Proc. Natl. Acad. Sci. U. S. A.* **1984**, *81*, 5412–5416.
- (70) Starr, F. W.; Nielsen, J. K.; Stanley, H. E. Fast and slow dynamics of hydrogen bonds in liquid water. *Phys. Rev. Lett.* **1999**, *82*, 2294–2297.
- (71) Fändrich, M. On the structural definition of amyloid fibrils and other polypeptide aggregates. *Cell. Mol. Life Sci.* **2007**, *64*, 2066–2078.
- (72) Toyama, B. H.; Weissman, J. S. Amyloid structure: Conformational diversity and consequences. *Annu. Rev. Biochem.* **2011**, *80*, 557–585.
- (73) Tsai, H.-H. G.; Zanuy, D.; Haspel, N.; Gunasekaran, K.; Ma, B.; Tsai, C.-J.; Nussinov, R. The stability and dynamics of the human calcitonin amyloid peptide DFNKF. *Biophys. J.* **2004**, *87*, 146–158.
- (74) Gazit, E. A possible role for π -stacking in the self-assembly of amyloid fibrils. *FASEB J.* **2002**, *16*, 77–83.
- (75) Sahoo, B.; Nag, S.; Sengupta, P.; Maiti, S. On the stability of the soluble amyloid aggregates. *Biophys. J.* **2009**, *97*, 1454–1460.
- (76) Pettersen, E. F.; Goddard, T. D.; Huang, C. C.; Couch, G. S.; Greenblatt, D. M.; Meng, E. C.; Ferrin, T. E. UCSF Chimera—A visualization system for exploratory research and analysis. *J. Comput. Chem.* **2004**, *25*, 1605–1612.